Optimization of cutting conditions in WEDM process using regression modelling and Tabu-search algorithm

M Sadeghi*, **H Razavi, A Esmaeilzadeh,** and **F Kolahan**
Ferdowsi University of Mashhad, Mashad, Iran

The manuscript was received on 5 January 2011 and was accepted after revision for publication on 21 March 2011.

DOI: 10.1177/0954405411406639

Abstract: The material removal rate (MRR) and surface roughness (SR) are the key output measures of wire electrical discharge machining (WEDM). In this paper, the influence of several process parameters, such as the discharge current, pulse interval, open-circuit voltage and servo voltage on the MRR and SR of WEDM, were investigated. Experimental data were initially collected based on the Taguchi method of experimental design. Modelling was carried out using regression analysis and the analysis of variance techniques, and mathematical relationships between the parameters and their related outputs were developed and tested. A Tabu search algorithm was then used to minimize a weighted sum of the outputs that represent different measures of machining quality and determine the optimal set of parameters for any combination of the weighting factors. The final results present the optimized MRR and SR of the process and confirm the efficiency and abilities of the model.

Keywords: wirecut, surface roughness, material removal rate, regression, analysis of variance, Tabu search

1 INTRODUCTION

Wire electrical discharge machining (WEDM) is a popular machining process for difficult-to-machine materials, many of which are widely used in tooling, especially in the aerospace and defence industries. In some particular cutting applications requiring high dimensional accuracy and high-quality surface finish, WEDM is one of the technical solutions available [**1**]. However, WEDM is a relatively slow process and hence has a low material removal rate (*MRR*), making it an expensive machining process [**2**]. Because the mechanism of material removal in WEDM is electro-discharge erosion by voltage pulses (as shown in Fig. 1), electrical parameters must be precisely adjusted to maximize the process efficiency. Improper parameter settings can cause short circuits, low-quality surface finish, and low *MRR* [**3**]. This sensitivity to process parameters has led to a great deal of discussion in the literature regarding the optimization of WEDM electrical characteristics [**4–21**].

The primary challenge to a thorough WEDM optimization model is the diversity of performance attributes and parameter settings. These are in turn applied to different work pieces and wire materials as well as process configurations. In fact, the diversity of materials and machining conditions used in WEDM makes research findings case-dependent and prevents comparison between different studies. In this research, a thorough background study has been performed, and different settings and approaches have been found and categorized in Table 1, which shows that over 12 years of research, WEDM optimization has been treated by a number of different techniques for a variety of parameters and workpiece materials.

It is obvious from Table 1 that the *MRR* and surface roughness (*SR*) are the characteristics most widely used to describe WEDM cutting conditions [**4–9**]. To establish a mathematical relationship between

**Corresponding author: Ferdowsi University of Mashhad, Mashhad, Iran.*
email: H.Sadeghi@ymail.com

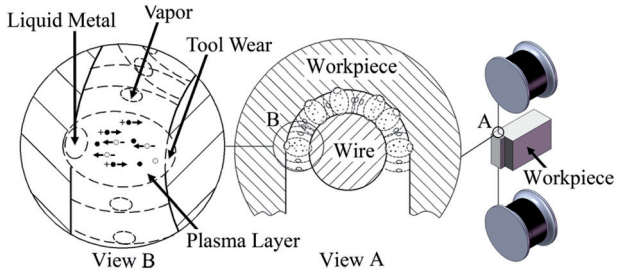

Fig. 1 Mechanism of WEDM material removal

WEDM input and output measures, both artificial neural networks and regression models have been applied [**10–15**]. Many optimization techniques have reported in technical papers, such as genetic algorithms and the Taguchi method [**16–19**]. Different steel alloys such as 1040, 2379, and 2738 steel have been investigated as workpiece materials [**20**]. WEDM also has some applications in metal-based composites. For instance, the effects of pulse duration, pulse interval, voltage and current on the output variables of Al_2O_3 particle reinforced 6061 aluminium alloy have been examined [**21**].

Owing to the importance of *MRR* and *SR* characteristics and their strong dependence on the input parameters, the paper was focused on them. As shown in Fig. 2, the input parameters of the model include the discharge current (I), pulse interval or time off (T_{off}), open-circuit (*OC*) voltage, and servo voltage (S).

Discharge current is directly proportional to crater size and the quantity of melted material, and the pulse interval affects the speed and stability of the process, i.e. it allows the molten material to solidify and be flushed out from the arc gap [**1**]. The remaining parameters are chosen based on the background studies listed in Table 1. Figure 3 illustrates the modelling and optimization procedures implemented in this research.

The regression model is preferred to artificial neural networks because of a number of disadvantages that neural networks present, including their black box nature, larger computational burden, proneness to over-fitting, and the empirical nature of neural network model development [**22**]. Thus, in this research, regression was utilized to model the WEDM process, and the Tabu search (TS) algorithm is adopted for the optimization. However, there is no evidence of any previous application of the TS technique, in spite of its benefits addressed in this paper.

In terms of workpiece material, AISI D5/DIN 1.2601 Steel was used because of its wide application in cutting tools, reamers, sockets, and heading dies. Moreover, there is no record of any previous investigations on this material at the input parameters shown in Fig. 2.

2 DESIGN OF EXPERIMENTS BY TAGUCHI METHOD

Initiating the procedure requires a set of experimental data. This initiation was performed using the Taguchi technique for a L_{16} (4^4) orthogonal array. The Taguchi approach to laying out experimental conditions significantly reduces the number of tests, overall testing time, cost of experiments, and the influence of nuisance factors and allows comparisons of mean treatment effects [**23**].

2.1 Tests and measurements

The physical WEDM tests were conducted on a CNC WireEDM machine (ONA Aricut R250 series 5-axis). The workpiece was a 30-mm-thick block of AISI D5/DIN 1.2601 Steel (X165CrMoV12), and the cutting brass wire was CuZn37 with a diameter of 0.25 mm and 900 N/mm^2 tensile strength. Next, 20-mm-long through cuts were made on the test pieces, and the cutting times were measured by a stopwatch. Then, the *MRR* was evaluated with the following equations:

$$F = \frac{60 \times l}{t} \tag{1}$$

$$MRR = F \times D_w \times H \tag{2}$$

where F is the average feed rate in mm/min, l is the cutting length in mm, and t is the cutting time in s. D_w is the wire diameter in mm, H is the work piece thickness in mm and *MRR* is thus measured in mm^3/min. When the cutting was complete, the surface finish was measured on a roughness-measuring machine (Mahr Perthometer M2), for three times on the same position. The final reported roughness R_a (in μm) of each sample is the average of these three measurements. Table 2 contains the measured results for 16 different arrays of parameters.

3 REGRESSION ANALYSIS

Mathematical relationships must be developed to describe the exact effects of different parameters on the performance measures. For this purpose, various regression functions were fitted and tested on the 14 sets of experimental data. Two rows (test no. 5 and 15) of the data in Table 2 were randomly left as control arrays for later evaluation of the functions.

Several linear and non-linear regression equations were used to model the objective function, and the best set of equations was then chosen based on two criteria: the R^2 test and the P-value [**24**]. Table 3 shows that the quadratic polynomial and nonlinear exponential models are the best fits for *MRR* and *SR*,

Table 1 Background studies

Year	Authors	Material		Input parameters	Performance measures	Solution technique
		Workpiece	Wire			
1999	Huang, J.T. *et al.* [**10**]	SKD11 Alloy steel	Brass	Pulse-on time, pulse-off time, table feed, flushing pressure, distance between wire periphery and workpiece surface, machining history	Gap width Surface roughness White layer depth	Taguchi, regression, feasible-direction algorithm
2000	Gökler, M. İ. and Ozanözgü, A. M. [**20**]	1040 steel, 2379 steel,2738 steel.	Brass	Voltage, current, time of cutting, average feed	Surface roughness	2D graph analysis
2002	Guo, Z. N. *et al.* [**21**]	Al_2O_3 particle reinforced	Brass	Pulse duration, pulse interval, voltage, current	Cutting rate Surface roughness	Orthogonal design
2003	Tosun, N. and Cogun, C. [**15**]	AISI 4140	CuZn37	Pulse duration, open-circuit voltage, wire speed, dielectric flushing pressure	The wire wear ratio Surface roughness	Regression, ANOVA
2004	Tosun, N. *et al.* [**17**]	AISI 4140 steel	Brass	Pulse duration, open circuit voltage, wire speed, dielectric flushing pressure	Kerf Material removal rate	Taguchi, regression, SA algorithm
2005	Kuriakose, S. H. and Shunmugam, M. S. [**16**]	Titanium alloy (Ti6Al4V)	Zinc-coated brass	Voltage, ignition pulse current, pulse-off time, pulse duration, servo-speed variation, wire speed, wire tension, injection pressure, servo-control reference mean voltage	Cutting velocity Surface finish	Regression, genetic algorithm, Pareto
2005	Sarkar, S. *et al.* [**18**]	γ-Titanium aluminide alloy	Brass	Pulse-on time, pulse-off time, peak current, servo reference voltage, wire tension, dielectric flowrate	Surface finish Dimensional accuracy Cutting speed	Taguchi, Pareto
2006	Chiang, K.T. and Chang, F. P. [**5**]	Al_2O_3 particle reinforced (6061 alloy)	Pure copper	On-time discharging, off-time discharging, arc-on time of discharging, arc-off time of discharging, servo voltage, wire feed, water flow, cutting radius of working piece	Material removal rate Surface roughness	Taguchi, grey relational analysis
2008	Mohammadi, A. *et al.* [**19**]	1.7131 Cemented steel	Brass	Power, time-off, voltage, wire speed, wire tension, rotational speed	Material removal rate	Taguchi, ANOVA, regression
2008	Yuan, J. *et al.* [**4**]	Chrome alloy Cr12	Molyb.	Mean current, on-time, off-time	Material removal rate Surface roughness	GPR, genetic algorithm, fuzzy clustering
2008	Sarkar, S. *et al.* [**13**]	γ-Titanium aluminide alloy	Brass	Pulse on time, peak current, flowrate, effective wire offset	Surface roughness Dimensional accuracy Cutting speed	RSM, ANOVA, Pareto
2008	Ramakrishnan, R. and Karunamoorthy, L. [**7**]	Inconel 718	Brass		Material removal rate Surface roughness	Artificial neural network, Taguchi.

(continued)

Table 1 Continued

Year	Authors	Material		Input parameters	Performance measures	Solution technique
		Workpiece	Wire			
2008	Haddad, M. J. and Tehrani, A. F. [**14**]	AISI D3 tool steel	Brass	Pulse-on time, delay time, wire feed speed, ignition current Power, pulse-off time, voltage, spindle speed	Material removal rate	Regression, ANOVA, RSM
2008	Sanchez, J A. *et al.* [**12**]	AISI D2 tool steel	CuZn20	Part thickness, taper angle, off-time, pulse energy, open-circuit voltage	Angular error	DOE, regression, FEM
2008	Ali, M. Y. and Mohammad, A. S. [**11**]	Copper	Brass	Discharge current, pulse-on time, gap voltage	Surface roughness Peak-to-valley height	DOE, regression
2008	Kung, K.Y. and Chiang, K.T. [**6**]	Aluminum oxide-based ceramic	Copper	Peak current, pulse on time, duty factor, wire speed	Material removal rate Surface roughness	CCD, RSM, ANOVA
2009	Rao, R. V. and Pawar, P. J. [**8**]	Oil hardened and nitrided steel (OHNS)	Brass	Pulse-on time, pulse-off time, peak current, servo feed setting	Machining speed Surface roughness	RSM, artificial bee colony (ABC)
2010	Jia, Y. *et al.* [**9**]	Polycrystalline diamond-coated tungsten carbide	Brass	Spark cycle, spark duration	Material removal rate Surface roughness	Design of experiment

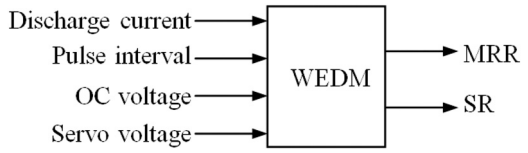

Fig. 2 Input and output parameters in this study

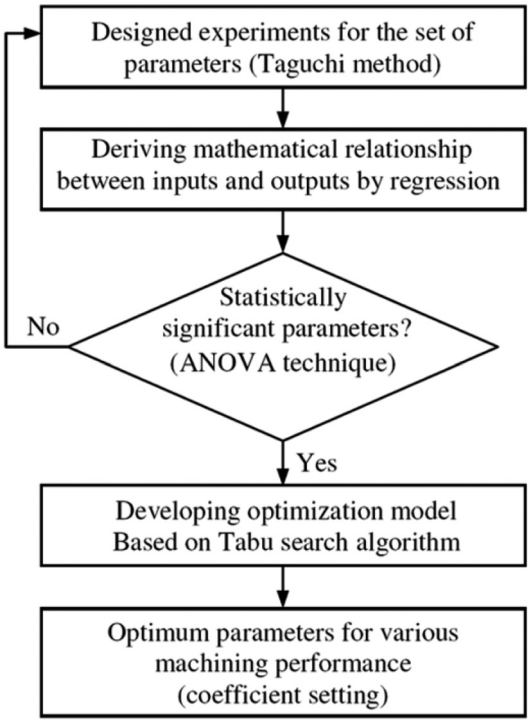

Fig. 3 Optimization flowchart

respectively, based on their R^2 values. The R^2 values indicate that the predictors explain 99.99 per cent of the *MRR* and *SR* variances.

Backward elimination was used to remove insignificant factors, according to the 95 per cent confidence level (*CL*), in the regression models, i.e. any factors with *P*-values higher than 0.05 were eliminated from the regression models. The finalized models are described by the following equations, which smoothly match the data points.

$$MRR = 23.9 + 23.2I - 9.87S - 0.744I^2 - 0.0333T^2 + 0.206S^2 - 0.103IT - 0.00535IV - 0.154IS + 0.0142TV - 0.00290VS \quad (3)$$

$$SR = \exp(1.99 + 0.360I - 0.0949T - 0.198S + 0.00492S^2 + 0.000012V^2 - 0.000588IV - 0.00788IS + 0.000484TV + 0.000919TS) \quad (4)$$

Using equations (3) and (4), the *MRR* and *SR* were calculated using the control parameter arrays. Figure 4 shows the comparison between the results of the fitted functions and the actual measurements. The average

Table 2 Experimental results

Exp. no.	Parameters: Discharge current (I) A	Pulse interval (T_{off}) μs	Open circuit voltage (V) V	Servo voltage (S) V	Surface roughness (SR) μm	Material removal rate (MRR) mm^3/min
1	9	8	140	32	3.270	9.593
2	9	10	120	30	2.845	8.205
3	9	14	110	26	2.421	7.725
4	9	22	130	28	2.575	6.000
5	10	8	120	28	3.046	10.913
6	10	10	140	26	3.035	12.255
7	10	14	130	30	3.018	11.108
8	10	22	110	32	2.745	6.698
9	11	8	110	30	3.229	12.645
10	11	10	130	32	3.410	13.875
11	11	14	140	28	3.169	12.555
12	11	22	120	26	2.707	7.995
13	12	8	130	26	3.528	14.288
14	12	10	110	28	3.293	12.435
15	12	14	120	32	3.462	11.033
16	12	22	140	30	3.408	8.250

estimation errors of the control samples were 7.1 per cent for *MRR* and 1.3 per cent for *SR*, which are acceptable levels for further applications.

4 ANALYSIS OF VARIANCE

Analysis of variance (ANOVA) is generally used to test for differences between datasets [**24**]. This method can also partition the total variance into components and investigate the effect of explanatory variables on the independent variables. A major assumption in ANOVA is the normality of the residuals. For the *MRR* and *SR* data in this research, the normality assumptions are confirmed as illustrated in Figs 5 and 6.

The critical region (*CR*) of the *F*-value at the 95 per cent *CL* for the *MRR* and *SR* is $F_{(0.05,3,3)} = 9.27$. As the ANOVA results for the *MRR* model in Table 4 indicate, the *F*-values of the discharge current, pulse interval and open circuit voltage were greater than the *CR* value and thus had statistically significant effects on *MRR*, but the servo voltage was not statistically significant. Therefore, the servo voltage must be pooled into the other parameters. Likewise, as Table 5 indicates, all parameters had statistically significant effects on *SR*.

The level at which each parameter contributes to the output variables can be verified by the ANOVA technique using equation (5).

$$\rho(\%) = \frac{SS_i - DF_i \times MS_e}{S_T} \tag{5}$$

where SS_i is the sum of squares for each parameter, DF_i is the degrees of freedom, MS_e is the mean squared error, and S_T is the total sum of squares. Figure 7 shows that the discharge current and pulse

Table 3 R^2 tests for regression models

Equation	R^2 (%): *MRR*	*SR*
Linear polynomial	93.7	98.84
Quadratic polynomial	99.99	99.95
Linear exponential	94.5	99.05
Nonlinear exponential	99.98	99.99

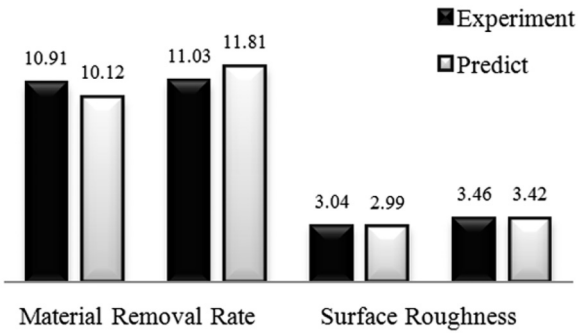

Fig. 4 Comparison of performance measures obtained theoretically and experimentally

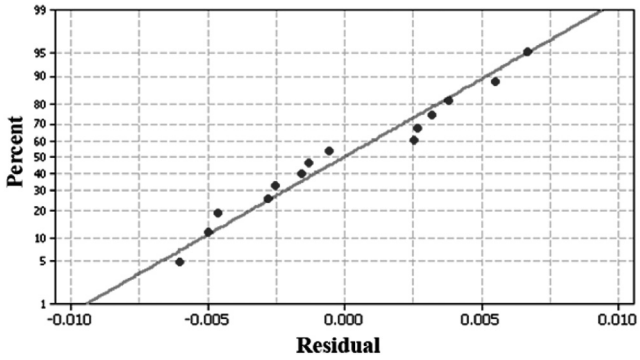

Fig. 5 Normality test on *MRR* results

interval have the highest percentage contribution, whereas the servo voltage is practically ineffective, with less than 1 per cent contribution.

Response surface methodology (*RSM*) can be used to analyse the simultaneous effect of explanatory variables on a response variable. The depiction of the cumulative effect of all four parameters on each performance measure needs a five-dimensional chart which is not practical. Therefore, pair-wise effects are assessed and plotted in three-dimensional charts. In particular, the mutual effect of the discharge current and pulse interval, two parameters suggested by *ANOVA*, are evaluated.

Figure 8 shows the mutual influence of the discharge current and pulse interval on the *MRR*. Higher *MRRs* are achieved at higher currents and shorter pulse interval.

Figure 9 shows the mutual influence of the same two parameters on the *SR* and shows that the surface roughness is optimized when the discharge current is lower and the intervals are longer. Concurrent analysis of all four parameters can be effectively performed using the TS algorithm.

5 TABU SEARCH ALGORITHM

Tabu search is a meta-heuristic algorithm that was first introduced by Glover [**25**]. The algorithm uses a stepwise search within the neighbourhood of each solution. Every solution that is obtained from the previous solution, even through a minor change, can be considered in the next step. In each iteration the objective functions are evaluated in different neighbourhoods and compared against each other. Therefore, moving from the current solution to the next, better solution becomes possible. This process continues until the stop conditions, such as computation time or number of iterations, are met.

After each iteration the previous solution is added to the Tabu list. The length of the Tabu list depends

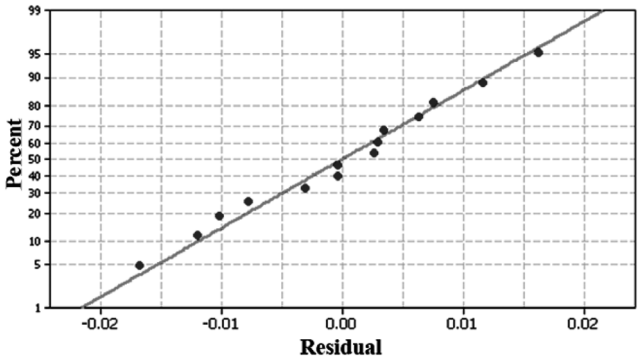

Fig. 6 Normality test on *SR* results

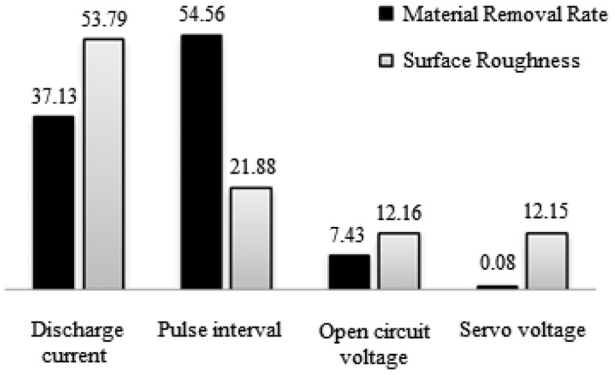

Fig. 7 Percentage contribution of each parameter

Table 4 ANOVA results for *MRR*

Source of variance	Degree of freedom (DF_i)	Sum of squares (SS_i)	Mean square (MS_i)	F-value (F)	P-value (P)
Discharge current	3	37.522	12.507	*85.73	0.000
Pulse interval	3	55.139	18.380	*125.98	0.000
Open circuit voltage	3	7.512	2.504	*17.16	0.002
Servo voltage	Pooled (3**)	Pooled (0.625**)	Pooled (0.208**)	Pooled (2.50**)	Pooled (0.229**)
Error	6	0.875	0.146	—	—
Total	15	101.048	—	—	—

*At least 95 per cent confidence.
**Value before pooling.

Table 5 ANOVA results for *SR*

Source of variance	Degree of freedom (DF_i)	Sum of squares (SS_i)	Mean square (MS_i)	F-value (F)	P-value (P)
Discharge current	3	0.89817	0.29939	23538.78	0.000
Pulse interval	3	0.36542	0.12181	9576.70	0.000
Open circuit voltage	3	0.20304	0.06768	5321.28	0.000
Servo voltage	3	0.20301	0.06767	5320.39	0.000
Error	3	0.00004	0.00001	—	—
Total	15	1.66967	—	—	—

*At least 95 per cent confidence.

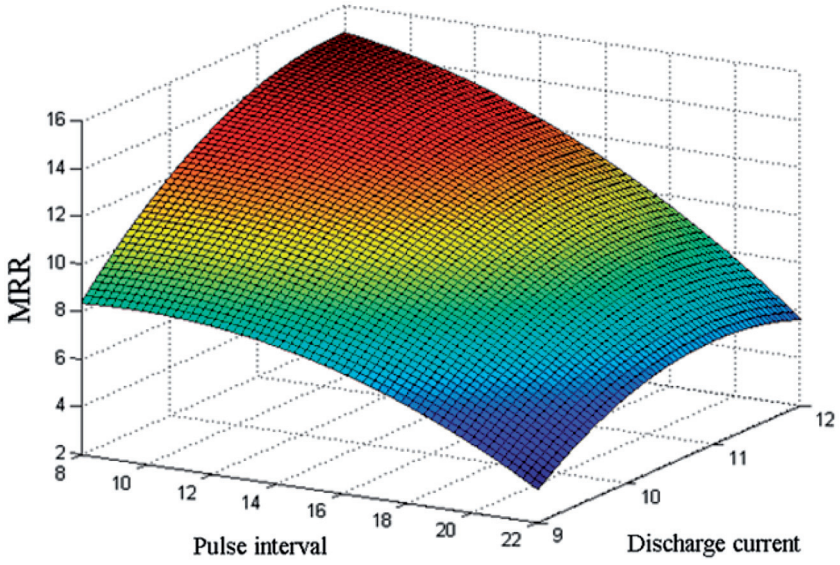

Fig. 8 Mutual effect of current and pulse interval on *MRR*

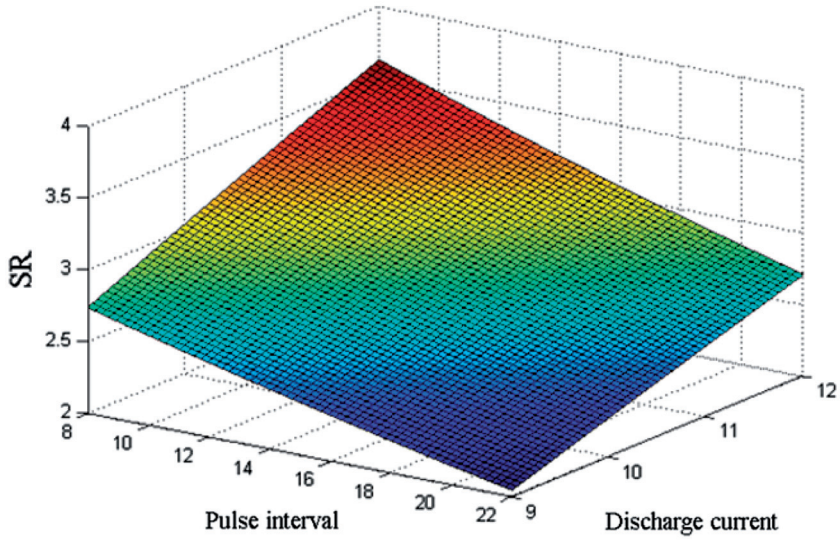

Fig. 9 Mutual effect of current and pulse interval on *SR*

on the nature of the problem and is empirically determined. The list contains the previously accepted solutions that are considered infeasible in the current iteration. This prevents the search from entering a closed loop so that the algorithm can expand the search space beyond the local neighbourhood.

A Matlab script was written based on the theory of TS for the current study. The script normalizes the equations and then uses a rated sum of attributes that relates rough, medium, or fine machining quality to corresponding *MRR* and *SR* levels. Because the *MRR* and *SR* of WEDM are counter-effective (i.e., increasing one decreases the other), each type of machining can be specified by an appropriate set of multipliers. The objective function is expressed by equation (6) [**26**].

$$\text{Min}(Z) = \omega_1 F_1^{\text{SC}} + \omega_2 F_2^{\text{SC}} \tag{6}$$

where ω_1 and ω_2 are the *MRR* and *SR* multipliers, respectively, and $\omega_1 + \omega_2 = 1$. Different machining performances can be modelled by varying ω_1. A higher ω_1 value will produce a greater *MRR* and reduced *SR*, resembling rough machining. Similarly, a higher ω_2 value enhances *SR* but reduces *MRR*, which is typical in fine WEDM.

Table 6 Optimization results

		Rough	Medium	Fine
Optimum machining condition		$\omega_1 = 1$; $\omega_2 = 0$	$\omega_1 = 0.5$; $\omega_2 = 0.5$	$\omega_1 = 0$; $\omega_2 = 1$
Parameters	Discharge current (A)	12	11	9
	Pulse interval (μs)	8	14	22
	OC voltage (V)	110	140	110
	Servo voltage (V)	26	26	26
Machining performance	*SR* (μm)	3.623	3.221	2.051*
	MRR (mm^3/min)	14.829*	14.190	3.392

*The optimized value.

The F_i^{SC} for $i = 1, 2$ are the normalized equations for *MRR* and *SR*, defined by equations (7) and (8).

$$F_1^{SC} = \frac{\left|F_1^* - F_1(x)\right|}{F_1^*} \tag{7}$$

$$F_2^{SC} = \frac{\left|F_2^* - F_2(x)\right|}{F_2^*} \tag{8}$$

where $F_i(x)$ functions are the same as in equations (3) and (4); and F_i^* for $i = 1, 2$ are the corresponding optimized values of $F_i(x)$. The two optimized values are obtained from running the Matlab program twice in advance. Equation (6) is then used in final running of the program to achieve the multi-objective optimization results. In the cases where one of ω_i is equal to zero, equation (6) will produce the same value as obtained in the pre run of the program. These values are identified in Table 6 by an asterisk (*).

5.1 Optimum results

The Matlab program was implemented on an Intel i5 processor and it took less than 3 s, which is fast enough for such cases. The results for three different machining qualities are summarized in Table 6.

The program returns a maximum *MRR* of 14.829 mm^3/min for rough machining and a minimum *SR* of 2.051 μm for fine machining (denoted by '*' in Table 6). To compare, the optimal *MRR* from Table 6 is 3.64 per cent greater than the maximum *MRR* in Table 2, and the optimal *SR* is 15.28 per cent less than the optimal *SR* in Table 2. These results provide evidence of the abilities of the program.

The optimal performance measures are obtained for parameter levels that do not occur in Table 2, proving that optimal parameter settings cannot be estimated through trial experiments even in a systematic approach. Table 6 also shows that the servo voltage is constant despite varying performance levels, supporting the findings in Section 4 that the *MRR* and *SR* are insensitive to this parameter.

6 CONCLUSION

The cost and quality of WEDM depend heavily on the process parameters. In this research, the effects of the discharge current, pulse interval, open-circuit voltage and servo voltage on the *MRR* and *SR* of WEDM were studied. The experimental data were collected from a slab made of cold steel 1.2601 in accordance with the Taguchi experimental design method. The *MRR* and *SR* were fitted to quadratic and exponential functions, respectively. The effect of each machining parameter on the *MRR* and the *SR* were determined using ANOVA. The discharge current and pulse interval were more influential on both the *MRR* and *SR* than the open-circuit voltage. The servo voltage had a smaller effect on the *SR* than the other parameters and no statistically significant effect on the *MRR*. The best set of models was then chosen based on the 95 per cent CL. The objective function of the model is the sum of the *MRR* and *SR* weighted by constant integrals of weighting multipliers. Any desired process performance can be defined by assigning proper values to the multipliers. The optimal input parameters can then be found using the TS algorithm. The final results for rough, medium and fine WEDM produced 3.64 per cent improvements in the *MRR* and 15.28 per cent in the *SR* compared to the values derived from systematic parameter setting.

FUNDING

This research received no specific grant from any funding agency in the public, commercial, or not-for-profit sectors.

ACKNOWLEDGEMENT

The authors would like to thank Mr H. Ramazy, from Isfehan University of Technology, for the experimental tests and results used in this project.

REFERENCES

1 **Oberg, E., Jones, F. D., Horton, H. L.,** and **Ryffel, H. H.** *Machinery's handbook*, 28th ed, 2008 (Industrial Press, New York).
2 **Brown, J.** *Advanced machining technology handbook*, 1998 (McGraw-Hill, New York).
3 **El-Hofy, H.** *Advanced machining processes*, 2005 (McGraw-Hill, New York).
4 **Yuan, J., Wang, K., Yu, T.,** and **Fang, M.** Reliable multi-objective optimization of high-speed WEDM process based on Gaussian process regression. *Int. J. Mach. Tools Manufact.*, 2008, **48**, 47–60.
5 **Chiang, K. T.** and **Chang, F. P.** Optimization of the WEDM process of particle-reinforced material with multiple performance characteristics using grey relational analysis. J. Mater. Process. Technol., 2006, **180**, 96–101.
6 **Kung, K. Y.** and **Chiang, K. T.** Modeling and analysis of machinability evaluation in the wire electrical discharge machining (WEDM) process of aluminum oxide-based ceramic. J. Mater. Manufact. Proc., 2008, **23**, 241–250.
7 **Ramakrishnan, R.** and **Karunamoorthy, L.** Modeling and multi-response optimization of Inconel 718 on machining of CNC WEDM process. J. Mater. Process. Technol., 2008, **207**, 343–349.
8 **Rao, R. V.** and **Pawar, P. J.** Modelling and optimization of process parameters of wire electrical discharge machining. *Proc IMechE, Part B: J. Engng Manufact.*, 2009, **233**, 1431–1440.
9 **Jia, Y., Kim, B. S., Hu, D. J.,** and **Ni, J.** Parametric study on near-dry wire electrodischarge machining of polycrystalline diamond-coated tungsten carbide material. *Proc IMechE, Part B: J. Engng Manufact.*, 2010, **224**, 185–193.
10 **Huang, J. T., Liao, Y. S.,** and **Hsue, W. J.** Determination of finish-cutting operation number and machining-parameters setting in wire electrical discharge machining. J. Mater. Process. Technol., 1999, **87**, 69–81.
11 **Ali, M. Y.** and **Mohammad, A. S.** Experimental study of conventional wire electrical discharge machining for microfabrication. J. Mater. Manufact. Proc., 2008, **23**, 641–645.
12 **Sanchez, J. A., Plaza, S., Ortega, N., Marcos, M.,** and **Albizuri, J.** Experimental and numerical study of angular error in wire-EDM taper-cutting. Int. J. Mach. Tools Manufact., 2008, **48**, 1420–1428.
13 **Sarkar, S., Sekh, M., Mitra, S.,** and **Bhattacharyya, B.** Modeling and optimization of wire electrical discharge machining of γ-TiAl in trim cutting operation. J. Mater. Process. Technol., 2008, **205**, 376–387.
14 **Haddad, M. J.** and **Tehrani, A. F.** Material removal rate (*MRR*) study in the cylindrical wire electrical discharge turning (CWEDT) process. J. Mater. Process. Technol., 2008, **199**, 369–378.
15 **Tosun, N.** and **Cogun, C.** Analysis of wire erosion and workpiece surface roughness in wire electrical discharge machining. *Proc IMechE, Part B: J. Engng Manufact.*, 2003, **217**, 633–642.
16 **Kuriakose, S. H.** and **Shunmugam, M. S.** Multi-objective optimization of wire-electro discharge machining process by non-dominated sorting genetic algorithm. J. Mater. Process. Technol., 2005, **170**, 133–141.
17 **Tosun, N., Cogun, C.,** and **Tosun, G.** A study on kerf and material removal rate in wire electrical discharge machining based on Taguchi method. J. Mater. Process. Technol., 2004, **152**, 316–322.
18 **Sarkar, S., Mitra, S.,** and **Bhattacharyya, B.** Parametric analysis and optimization of wire electrical discharge machining of γ-titanium aluminide alloy. J. Mater. Process. Technol., 2005, **159**, 286–294.
19 **Mohammadi, A., Tehrani, A. F., Emanian, E.,** and **Karimi, D.** Statistical analysis of wire electrical discharge turning on material removal rate. J. Mater. Process. Technol., 2008, **205**, 283–289.
20 **Gökler, M. İ.** and **Ozanözgü, A. M.** Experimental investigation of effects of cutting parameters on surface roughness in the WEDM process. Int. J. Machine Tools Manufact., 2000, **40**, 1831–1848.
21 **Guo, Z. N., Wang, X., Huang, Z. G.,** and **Yue, T. M.** Experimental investigation into shaping particle-reinforced materials by WEDM-HS. J. Mater. Process. Technol., 2002, **129**, 56–59.
22 **Hu, Y. H.** and **Hwang, J. N.** *Handbook of neural network signal processing*, 2002 (CRC Press, New York).
23 **Roy, R.** *A primer on Taguchi method*, 1990 (Van Nostrand Reinhold, New York).
24 **Montgomery, D. C.** *Design and analysis of experiments*, 7th ed, 2008 (Wiley, New York).
25 **Glover, F.** and **Laguna, M.** *Tabu search*, 1997 (Kluwer Academic, Dordrecht).
26 **Miettinen, K.** *Nonlinear multiobjective optimization*, 1999 (Kluwer Academic, Boston).

APPENDIX

Notation

DF_i	degree of freedom (i = 1,. . ., 4)
D_w	wire diameter (mm)
F	average feed rate (mm/min)
F_i^*	optimized values for MRR and SR (i = 1, 2)
F_i^{SC}	normalized equations for MRR and SR (i = 1, 2)
$F_i(x)$	the MRR and SR equations (i = 1, 2)
H	workpiece thickness (mm)
I	discharge current (A)
L	cutting length (mm)
MRR	material removal rate (mm^3/min)
MS_e	mean squared error
Q	percentage contribution (%)
R^2	correlation coefficient
R_a	arithmetic mean of the roughness profile (μm)
S	servo voltage (V)
SR	surface roughness (μm)
SS_i	sum of squares (i = 1,. . ., 4)

S_T	total sum of squares
T	cutting time (s)
T_{off}	pulse interval (μs)
V	open circuit voltage (V)
ω_i	the MRR and SR multipliers (i = 1,2)
Z	objective function

Abbreviations and definitions

ANOVA	analysis of variance
CL	confidence level
CR	critical region
F	F-value
P	P-value
RSM	response surface methodology
TS	Tabu search algorithm
WEDM	wire electrical discharge machining